Supporting Information

Zirconium-based MOF nanocrystals confined on amphoteric halloysite nanotubes for promoting catalytic hydrolysis of organophosphorus nerve agent simulant

Shuwen Li, Heyao Zhang, Gaigai Wu, Jie Wu, Hongwei Hou**

Green Catalysis Center, College of Chemistry, Zhengzhou University, Zhengzhou 450001, P. R. China.

Chemicals and Instrumentation

Materials

All reagents were purchased from commercial sources and used without further purification.

Zirconium (IV) oxychloride octahydrate ($ZrOCl_2 \cdot 8H_2O$), Zirconium chloride ($ZrCl_4$), formic acid (HCOOH), acetic acid (CH_3COOH), 2-aminoterephthalic acid.

Characterization

Powder X-ray diffraction (PXRD) patterns were measured by Bruker Advance D8 Powder X-ray diffractometer with Ni-filtered Cu Kα radiation. Crystals were scanned from 2° to 70° with 0.01° steps at 40 kV and 40 mA. Scanning electron microscopy (SEM) images of samples were taken using Zeiss Sigma 500. Transmission electron microscopy (TEM) images were analyzed using jem 2100. Fourier transform infrared (FT-IR) spectroscopy was performed within the range 4000-400 cm^{-1} on a Bruker Vector 22 spectrophotometer by KBr pellets. N_2 adsorption-desorption was conducted by automatic volumetric adsorption equipment (BelsorpMax) at 77 K. All samples were activated under vacuum at 120 °C for 12 h. Thermogravimetric analysis (TGA) was obtained using Netzsch STA 449C thermal analyzer between 30 °C and 800 °C at a heating rate of 10 °C/min. In-situ ^{31}P NMR experiments were carried out on a Bruker Avance-400 spectrometers.

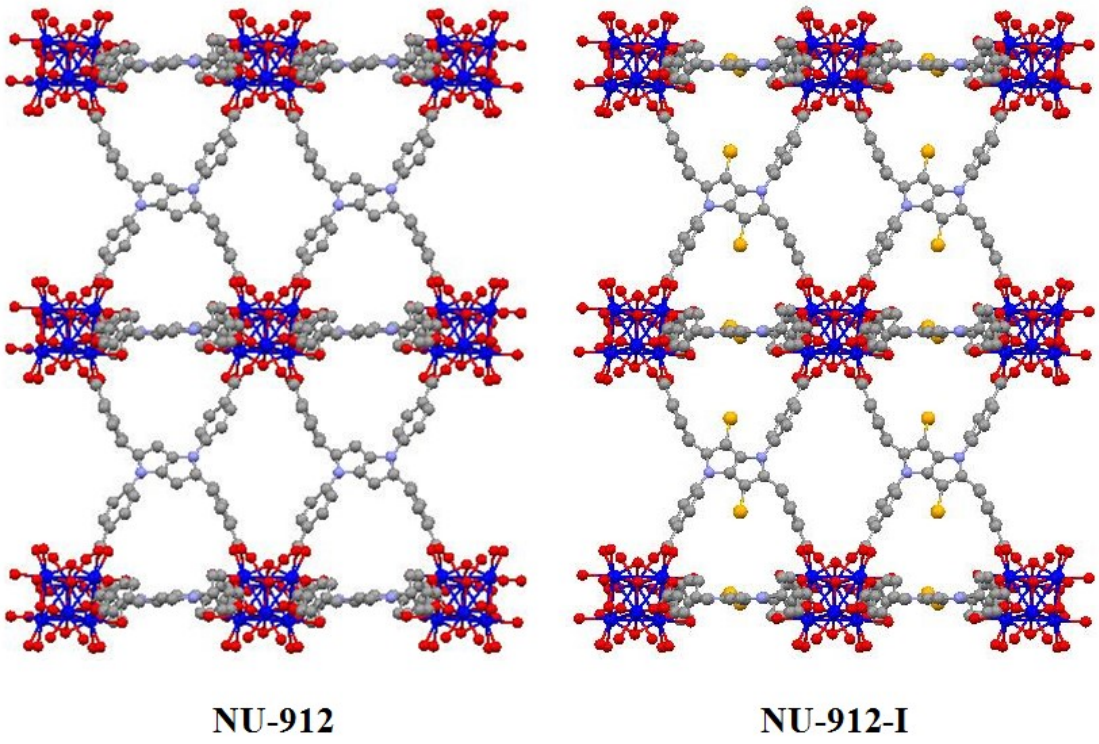

Figure S1. Framework diagram of NU-912 and NU-912-I.

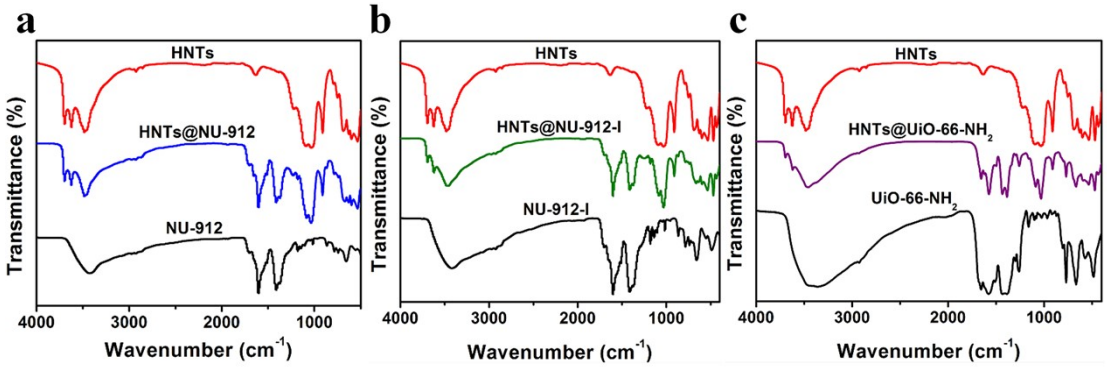

Figure S2. FT-IR spectra of (a) HNTs@NU-912, (b) HNTs@NU-912-I, and (c) HNTs@UiO-66-NH_2.

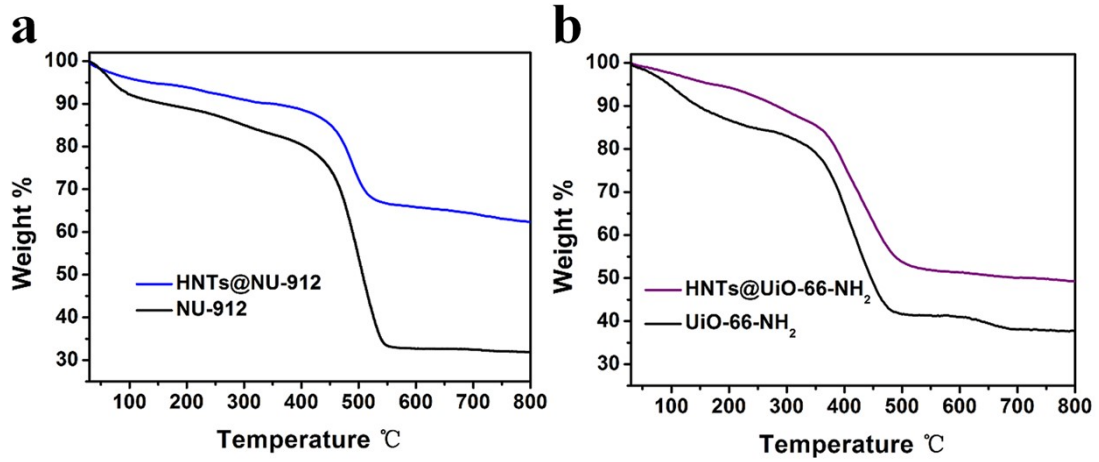

Figure S3. TGA curves of (a) HNTs@NU-912 and (b) HNTs@UiO-66-NH_2.

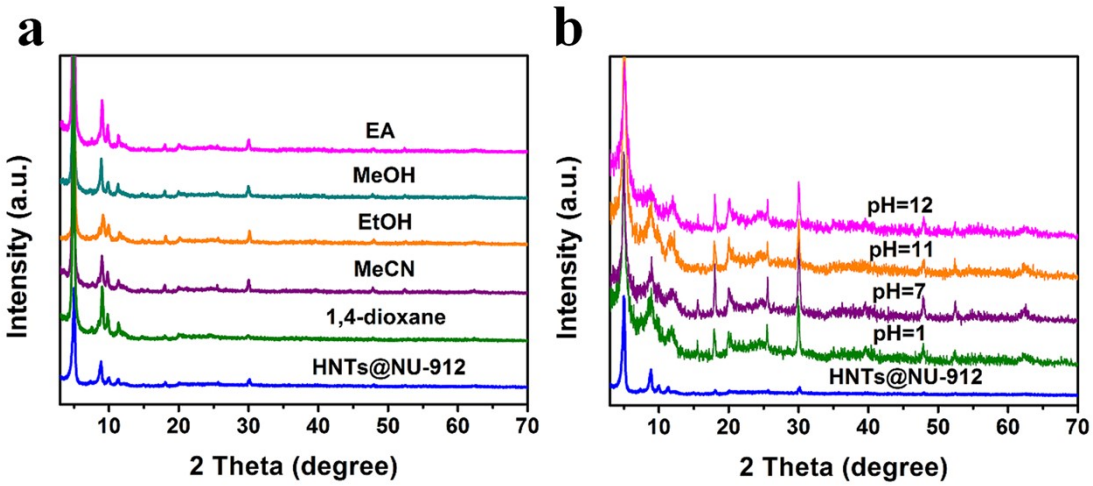

Figure S4. PXRD patterns of (a) HNTs@NU-912 after immersing in different organic solvents and (b) aqueous solutions with pH=1-12 for about 24 h.

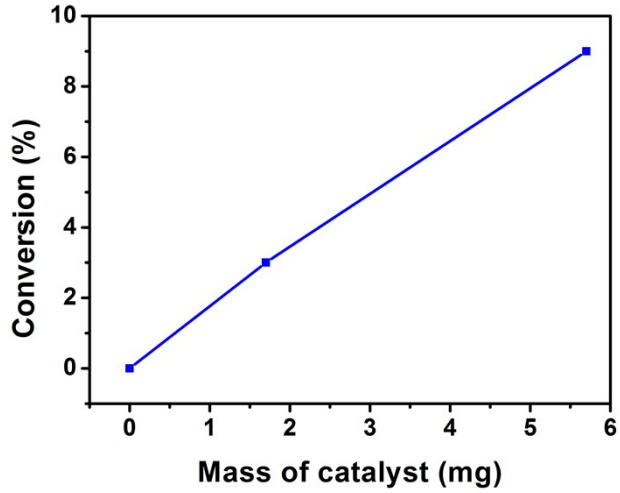

Figure S5. Conversion profile for the liquid-state hydrolysis of DMNP by HNTs@NU-912 in the absence of NEM afetr 1 h.

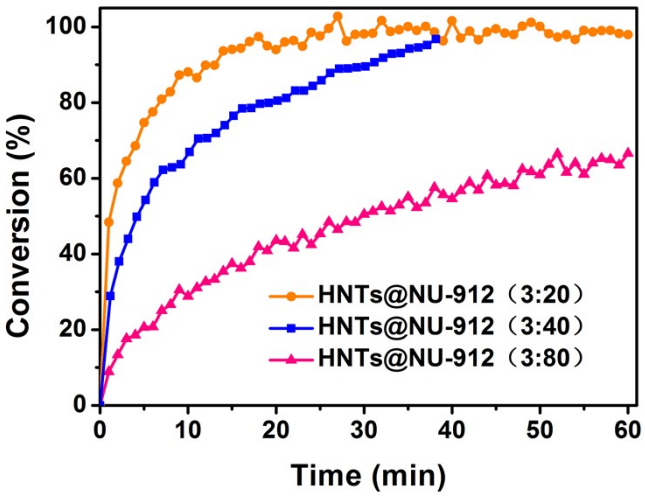

Figure S6. Hydrolysis profiles of DMNP by HNTs@NU-912 with different molar ratios in aqueous base solution.

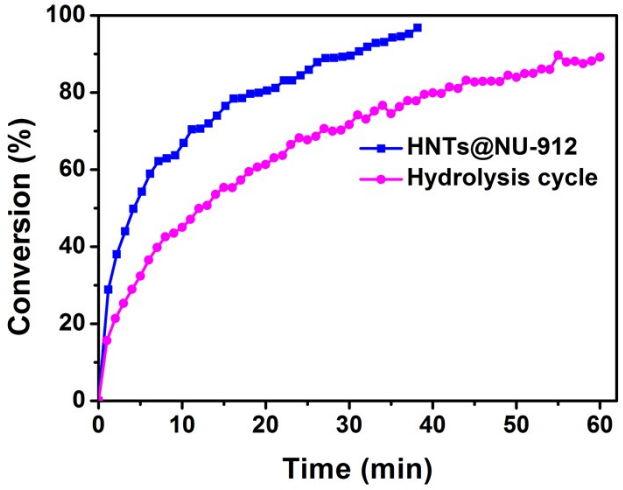

Figure S7. After hydrolysis, HNTs@NU-912 was washed and dried and reused for DMNP hydrolysis.

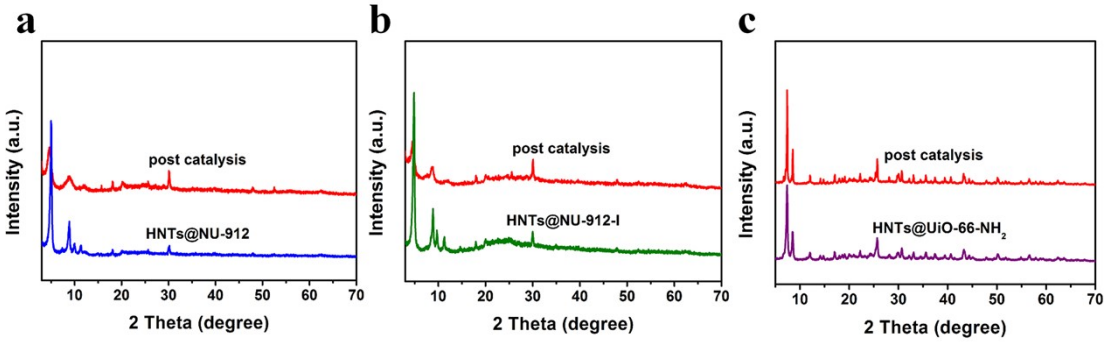

Figure S8. PXRD patterns of (a) HNTs@NU-912, (b) HNTs@NU-912-I, and (c) HNTs@UiO-66-NH_2 after catalytic reaction.

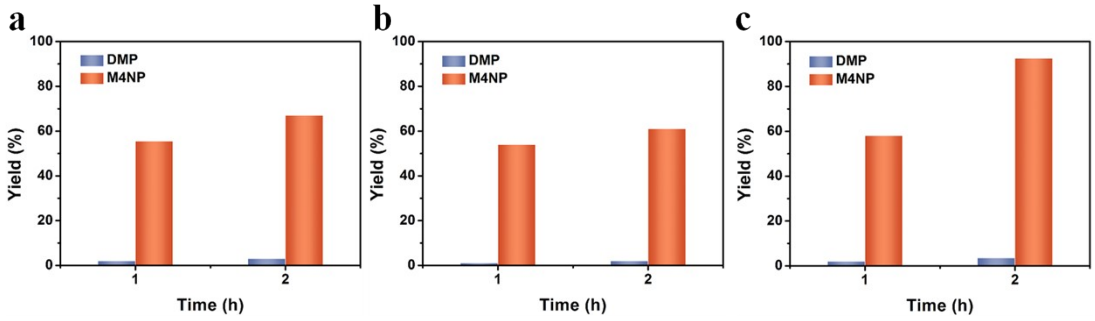

Figure S9. Solid-state hydrolysis yield of DMNP with (a) NU-912, (b) NU-912-I, (c) UiO-66-NH_2 in PEI solution under RH = 99% (catalysts: 6 mol%, DMNP: 4 μL, 0.025 mmol, PEI: 16.3 mg).